

Assessing Hydrological Drought in the Nekor Watershed Using the Streamflow Drought Index: Patterns, Trends, and Implications

Abdelmonaim Okacha^{1*}, Adil Salhi¹, Kamal Abdelrahman², Kamal Lahrichi³,
Hamid Fattasse³, Mounir Bouchouou¹, Biraj Kanti Mondal⁴

¹ Geography Department, Abdelmalek Essaadi University, Martil, B.P. 210, Morocco

² Geology Department, King Saud University, Riyadh, 11451, Saudi Arabia

³ Geography Department, Sidi Mohamed Ben Abdellah University, Fez, 30000, Morocco

⁴ Geography Department, School of Sciences Netaji Subhas University Kolkata, West Bengal, 700090 India

* Corresponding author's e-mail: okacha1abdelmonaim@gmail.com

ABSTRACT

The Nekor Watershed, situated in the northwest corner of Africa, experiences significant climatic variability, posing challenges for water management. This study assesses hydrological drought in the Nekor Watershed from 1945 to 2016 and analyzes its socio-economic impacts on agriculture and population distribution. The purpose of this research is to understand the extent and trends of hydrological drought in the Nekor Watershed and its socio-economic consequences, particularly on agriculture and population dynamics. The study employs the Standardized Runoff Efficiency Index (SDI), drought duration, severity (S), magnitude (M), and relative frequency (RF) metrics, along with the Mann-Kendall trend test and Sen's Slope analysis to evaluate hydrological drought. It integrates statistically representative data on cereal crop yields, livestock populations, and results from the General Population and Housing Census to understand the socio-economic impacts. Analysis reveals substantial climatic variability with pronounced dry and wet periods. Notably, the autumn season exhibits a weak positive trend in hydrological drought, indicating a slight increase in severity over the years. Conversely, the spring season shows a negative trend in hydrological drought, indicating a decrease in severity over the years, especially in the month of May. A broader trend towards increasing hydrological drought emerges, particularly since the 1980s. These dry decades pose significant challenges for the region's socio-economic sectors, including agriculture and population distribution. The study is limited by the availability and quality of historical hydrological and socio-economic data, which may affect the precision of trend analyses and impact assessments. Future research could benefit from more granular and continuous data sets. Understanding the trends and impacts of hydrological drought in the Nekor Watershed provides critical insights for water management policies and strategies, helping to mitigate socio-economic risks associated with drought. This study is novel in its comprehensive analysis of long-term hydrological drought trends in the Nekor Watershed and their socio-economic impacts. The integration of diverse data sets and advanced statistical methods enhances the robustness of the findings, contributing significantly to the scientific understanding of drought dynamics in this region.

Keywords: climate change, hydrological drought, patterns, trends, Nekor Watershed, Africa.

INTRODUCTION

The impact of climate change has begun to exceed expected levels worldwide, particularly evident in the increased occurrence and severity of droughts. Drought, a natural disaster, is internationally recognized and defined by varying parameters depending on its impact and the

scientific discipline [Değerli Şimşek et al., 2023; Fan et al., 2017; Maybank et al., 1995]. Meteorologists characterize drought as an extended absence, significant deficit, or spatially uneven distribution of precipitation compared to a defined norm. Hydrologically, it manifests as a prolonged meteorological drought causing a sudden decline in groundwater levels, rivers, streams, and lakes.

Agriculturally, drought denotes a marked and persistent deficit in rainfall impacting agricultural production estimated based on an average value. Socio-economically, it is identified by insufficient rainfall with detrimental effects on the local population and regional economy. With the recent escalation of global warming, significant shifts are occurring in hydrometeorological parameters such as precipitation, flow, and temperature [Li et al., 2011; Polevoy et al., 2024; Redner and Petersen, 2006]. This crisis also influences other hydrological variables like evaporation, with increased evaporation events leading to drier periods. Upon detection of drought in a region, early disparities emerge in precipitation data, signaling the onset of meteorological droughts, followed by agricultural and ultimately hydrological droughts.

In semi-arid regions, precipitation quantity stands as one of the most fundamental factors supporting livelihoods [Qaisrani et al., 2018]. Substantial changes in precipitation values must be carefully considered for both habitation zones and continued agricultural activities. Consequently, meteorological and hydrological data fluctuations necessitate thorough examination to address agricultural, industrial, and domestic water needs [Zhou et al., 2024].

Following the advancements of the 20th century, which saw the introduction of the Cradock Precipitation Index, De Martonne's Aridity Index [De Martonne, 1923], and the Thornthwaite potential evapotranspiration index (PEPI) [Thornthwaite, 1948], drought monitoring has become an increasingly crucial practice in the face of climate change. Rising global temperatures are believed to be altering precipitation patterns, impacting water resource availability and potentially leading to more frequent floods and droughts. Studies suggest an anticipated increase in droughts due to these changes, necessitating the frequent use of robust drought indices for effective assessment. Among the noteworthy advancements in drought monitoring tools are the standardized melt and rainfall index (SMRI) [Staudinger et al., 2014], the standardized streamflow index (SSI) [Modarres, 2007; Zaidman et al., 2002], the standardized precipitation and evapotranspiration index (SPEI) [Serrano et al., 2010], and the soil moisture index (SMI) [Sridhar et al., 2008]. However, the Standardized Precipitation Index (SPI) [McKee et al., 1993] remains widely used. The Hydrological Drought Index (SDI), derived from the SPI by Nalbantis and Tsakiris [2009], plays

a particularly pivotal role. This powerful tool leverages monthly river flow data to delineate and evaluate hydrological droughts with greater precision and rigor. The SDI's practicality has led to its frequent utilization in recent studies. It is calculated using the mean and standard deviation of observed streamflow data, enabling the classification of drought and rainfall durations. Additionally, the SDI's ability to detect potential gaps in precipitation trends using streamflow data is expected to have positive implications for water resource planning procedures, particularly regarding cost-effectiveness.

Morocco experiences significant climate variability, making it highly vulnerable to droughts [Abdelmajid et al., 2021; Snaibi et al., 2021]. These droughts profoundly impact the country's agriculture, water resources, and socio-economic conditions [Gaaloul et al., 2021; Zahour, 2021]. Researchers have employed various indices to assess and monitor drought conditions. In recent studies, Amouch and Akhssas [2023] assessed drought variability from 1973 to 2020 and projected future conditions up to 2099 using the Standardized Precipitation Index (SPI). They identified 1981-1986 as the driest period and projected future prolonged droughts, while examining rainfall-NAO relationships to improve drought management. Meliho et al. [2020] studied the Tensift watershed in mid-west Morocco, using SPI to demonstrate the impact of drought on Takerkoust dam inflows and N'Fis agricultural production, which led to significant irrigation and crop reductions. Elair et al. [2023] analyzed drought in the Marrakech-Safi region from 1980 to 2018, using SPI and remote sensing indices (VCI, TCI, VHI). They found increasing drought trends, especially in autumn, with significant vegetation sensitivity. The dominant feature of these studies is their relatively short study periods and their reliance on rainfall-based indicators.

This research aims to comprehensively assess hydrological drought in the Nekor Watershed in the context of the climate change, specifically focusing on the Rif centro-eastern region, a crucial agricultural basin. By analyzing recurring drought patterns (frequency, duration, intensity) and trends in drought occurrences (potentially increasing or decreasing severity) using total flow data (1945–2016) from the Tamellaht station, we will evaluate the resulting socio-economic impacts on agriculture and demography. The study employs the standardized runoff efficiency index

(SDI) calculated across monthly, seasonal, and annual intervals to highlight the probability of drought and wet periods. We expect these findings to significantly contribute to current drought literature and inform future emergency action plans for the region.

METHODS

Building upon the conceptual framework of the standardized precipitation index (SPI), the streamflow drought index (SDI) was introduced by Nalbantis and Tsakiris [2009] to characterize hydrological droughts. In Morocco, the hydrological year spans from September to August of the following year. To capture different temporal scales and ensure robust analysis, four overlapping time periods, referred to as reference periods, are

employed within each hydrological year: Monthly, seasonal (a quarter of a hydrological year), and September to August (hydrological year).

Study area

This study focuses on the Nekor watershed, a 691 km² basin (at Tameiaht station) located in northeastern Morocco (Figure 1). Its geographical coordinates range from 34°69' to 35°19' North latitude and 3°36' to 4° West longitude. The watershed experiences a Mediterranean climate characterized by hot, dry summers and mild, wet winters. However, its upstream areas exhibit a continental influence and are subject to the Foehn effect [Okacha et al., 2023; Salhi et al., 2019]. This phenomenon occurs when moist air masses rise over mountains, cool, condense, and release precipitation on the windward side. As the

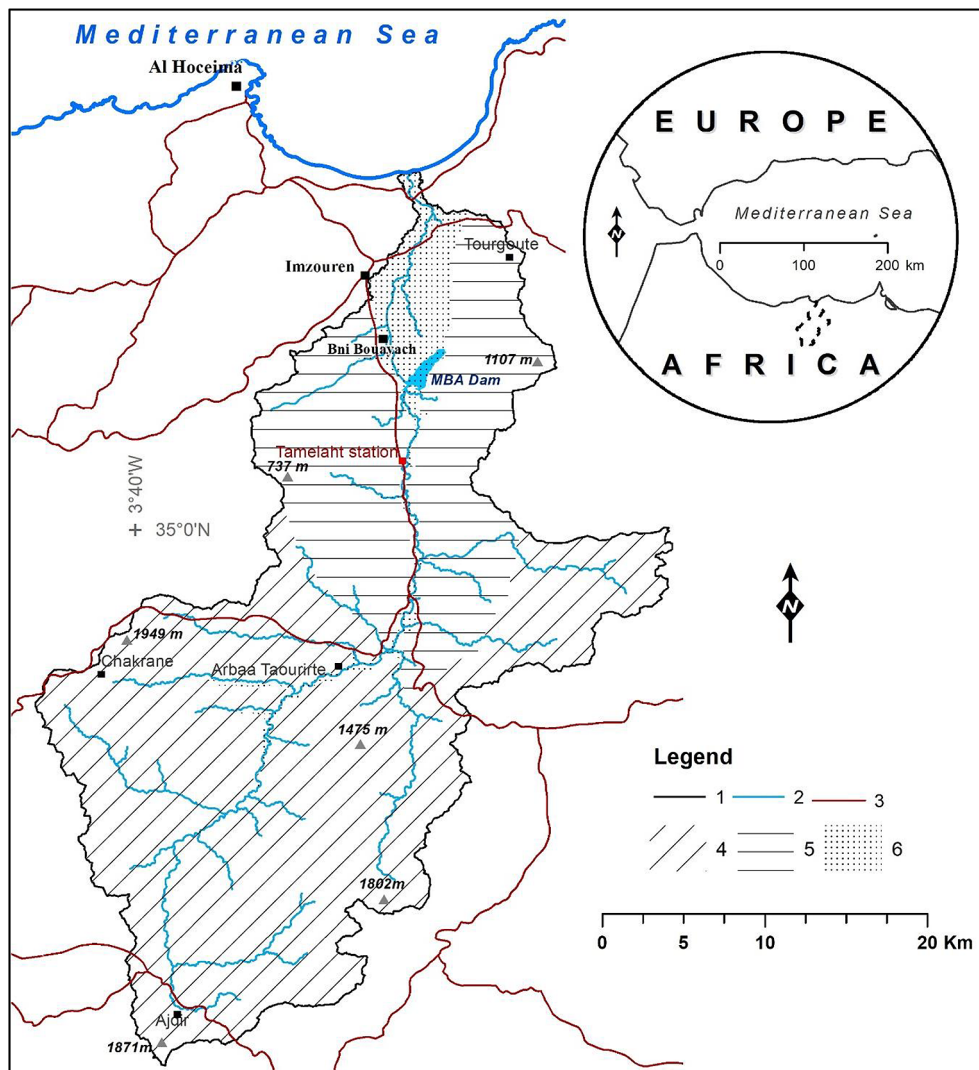


Figure 1. Location of the study area. 1 – Nekor watershed, 2 – River Network, 3 – Road Network, 4 – High folded mountains, 5 – Hills, and low mountains, 6 – Nekor plain

air descends on the leeward side, it warms and dries, leading to increased aridity in the upstream regions of the Nekor watershed [Okacha, 2020].

The Nekor watershed is characterized by significant climatic variability, with a disturbing trend towards aridification. This trend is exacerbated by the Foehn effect, leading to increasingly frequent droughts, particularly in the upstream areas. These fluctuating and unpredictable climatic conditions significantly impact the region’s water resources, agricultural productivity, and local ecosystems. Consequently, the Nekor watershed presents a critical case study for investigating hydrological drought and its socio-economic ramifications.

Data

This study utilizes a combination of topographical, hydrological, socio-economic, and demographic data to assess historical trends in hydrological conditions and their impacts within the Nekor Watershed, Morocco (Figure 1).

Topographical data

A 12-meter resolution digital elevation model (DEM) for the Nekor Watershed from the year 2020 is included in the study to delineate topographic units within the watershed, GDEM dataset is available in <https://asterweb.jpl.nasa.gov> (Table 1).

Hydrological data

The primary source of hydrometric data is monthly hydrometric readings from the Tamellaht station (1944–2016) (Figure 2), located within the Nekor Watershed (Figure 1). This station, managed

by the Loukous Hydraulic Agency, monitors a drainage area of 691 km². These data are utilized for calculating the cumulative streamflow volume $V(i, k)$ (Equation 1) and the streamflow drought index (Equation 2) across various timescales, including monthly, seasonal, and annual analyses.

Socio-economic and demographic data

To assess the socio-economic and demographic consequences of drought events, the study incorporates data from various sources (Table 1):

Crop yields (quintals/hectare): Statistical data on cereal crop yield evolution within the watershed (1960–1969 and 2007–2014). Data sources include Bossard (1978) for Tamsamane and Bni Touzine tribes and the Regional Directorate of Tanger-Tétouan-Al Hoceima for Al Hoceima province.

Livestock populations: Data on livestock populations within Al Hoceima province (1978–1989) obtained from MARA (cited by El Sabri, 1995).

Population data: Population data for Arbaa Tourirt coumune and each topographic unit of the Nekor Watershed for the years 1960, 1971, 1982, 1994, 2004, and 2014. This data is sourced from the general population and housing censuses (RGPH) conducted by Moroccan state institutions.

Streamflow data preparation

The calculation of the SDI relies on a time series of monthly streamflow volumes denoted by $Q(i, j)$. Here, i represents the hydrological year (e.g., starting in September and ending in August) and j represents the month within that year (ranging from 1 for September to 12 for August).

Table 1. Data sources for hydrological, socioeconomic, and demographic analysis in study area

Category	Type	Year or period	Zone	Sources
Topography	12 m resolution GDEM	2020	Nekor watershed	https://asterweb.jpl.nasa.gov
Hydrometric	Monthly	1944–2016	Tamellaht station	Loukous Hydraulic Agency
Socio-economic	Crop yields (quintals/hectare)	1960–1969	Tamsamane and Bni Touzine tribes	Bossard [1978]
	Livestock populations	1978–1989	Al Hoceima province	MARA, cited by El Sabri [1995]
	Crop yields (quintals/hectare)	2007–2014	Al Hoceima province	Regional Directorate of Tanger-Tétouan-Al Hoceima
Demographic	Population data	1960, 1971, 1982, 1994, 2004, 2014	Arbaa Tourirt coumune and each unit topographic of Nekor watershed	General Population and Housing Census (RGPH)

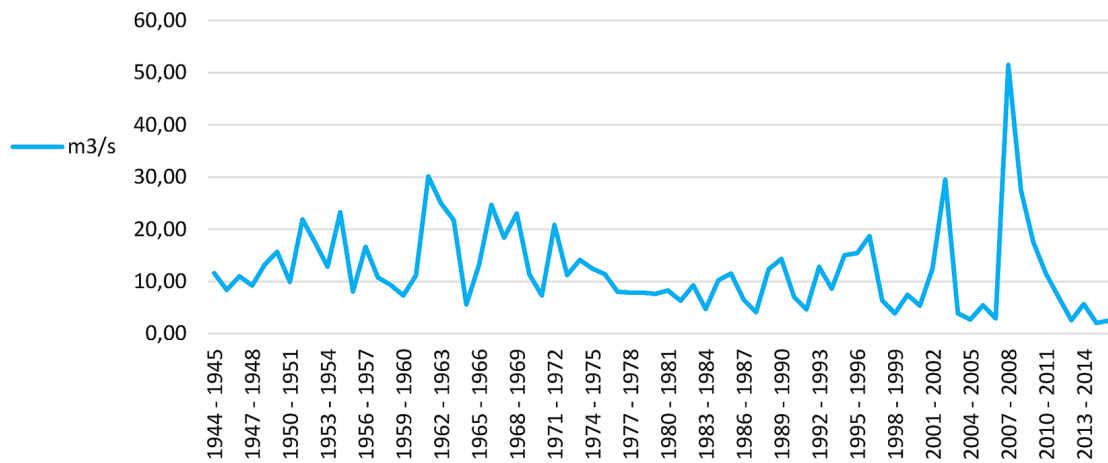


Figure 2. Evolution of Annual Streamflow (m³/s) at Tamellahte Station (1944–2016)

Calculation of cumulative streamflow volume

For each hydrological year i , the cumulative streamflow volume $V(i, k)$ is computed for different reference periods k using the following Equation 1:

$$V(i, k) = \sum_{j=start(k)}^{end(k)} Q(i, j) \quad (1)$$

where: $Q(i, j)$ represents the streamflow for month j within hydrological year i .

Reference periods (k): This defines different timeframes used to assess streamflow accumulation. Here's a breakdown of the reference periods:

- Monthly ($k = m$): This is the most granular level, considering a single specific month (m) as the reference period. Both the starting and ending month ($start(k)$ and $end(k)$) are simply equal to the chosen month (m).
- Seasonal ($k = s$): This considers seasonal variations in streamflow. There are four sub-categories within the seasonal reference period:
 - o Autumn (September to November): For this season (s), the starting month ($start(k)$) is set to 1 (September) and the ending month ($end(k)$) is set to 3 (November).
 - o Winter (December to February): The winter season (s) uses a starting month ($start(k)$) of 4 (December) and an ending month ($end(k)$) of 6 (February).
 - o Spring (March to May): Spring (s) starts at month 7 (March) ($start(k)$) and ends in month 9 (May) ($end(k)$).
 - o Summer (June to August): The summer season (s) begins in month 10 (June) ($start(k)$) and concludes in month 12 (August) ($end(k)$).

- Annual ($k = \text{entire year}$): This considers the entire hydrological year as the reference period. In this case, both the starting ($start(k)$) and ending month ($end(k)$) are set to 12, representing the full hydrological year.

Streamflow drought index (SDI) calculation

The SDI for each reference period k of the i -th hydrological year is determined based on the cumulative streamflow volume $V(i, k)$ using the following Equation 2:

$$SDI(i, k) = \frac{(V(i, k) - V_k)}{S_k} \quad (2)$$

where: V_k represents the long-term average (mean) of the cumulative streamflow volume for the reference period k . S_k represents the standard deviation of the cumulative streamflow volume for the reference period k , calculated over a long historical period.

The hydrological drought index defined in Equation 2 is essentially a standardized streamflow volume, a concept initially explored by Ben-Zvi [1987], who used standardized annual streamflow volumes. Ben-Zvi defined a “deep shortage” as an annual streamflow volume that is at least one standard deviation below the mean. However, his work did not address non-stationarity, as he focused solely on annual data [Nalbantis and Tsakiris, 2009]. In this study, for the Nekor watershed, streamflow exhibits a skewed probability distribution, which is well approximated by Gamma distribution functions. This distribution is subsequently transformed into a normal distribution for analysis.

Fitting gamma distribution

The cumulative streamflow volumes $V(i, k)$ are fitted to a Gamma distribution, as streamflow data typically exhibits a skewed probability distribution. The parameters of the Gamma distribution, shape (α) and scale (β), are estimated using the Moment method. the shape and scale parameters can be estimated as follows:

Shape parameter (α):

$$\alpha = \frac{\mu^2}{\sigma^2} \tag{3}$$

Scale parameter (β):

$$\alpha = \frac{\sigma^2}{\mu} \tag{4}$$

where: μ is the sample mean and σ^2 is the sample variance. These formulas are derived by setting the first and second moments of the sample equal to the first and second moments of the Gamma distribution.

Transformation to standard normal distribution

The cumulative distribution function (CDF) of the fitted Gamma distribution is used to transform the streamflow data into a standard normal distribution. This transformation is given by:

$$Z = \Phi^{-1}(G(V(i, k))) \tag{5}$$

where: Z now represents the standardized SDI, G is the CDF of the Gamma distribution, Φ^{-1} is the inverse of the standard normal CDF, $V(i,k)$ is the cumulative streamflow volume.

Interpretation of SDI values

Positive SDI values indicate wetter than average conditions for the corresponding reference period. Conversely, negative values signify a

hydrological drought. The SDI exhibits a range of wetness and dryness spanning from -2 to +2, as detailed in Table 2.

Drought characterization

The SDI, along with its time series analysis, allows for the characterization of droughts based on various parameters:

- Drought duration (D): This refers to the length of time a drought persists. It is calculated as the period between the start (first occurrence of a negative SDI value) and end (first occurrence of a positive SDI value) of a drought event.
- Drought severity (S): This parameter quantifies the intensity of a drought event. It is calculated by summing the negative SDI values within the drought duration. The Equation 6 for drought severity is as follows:

$$S = \sum SDI(i, k) \tag{6}$$

where: S represents the drought severity, $SDI(i, k)$ represents the SDI value for the i -th hydrological year and the k -th reference period

The summation iterates over all negative $SDI(i, k)$ values within a single drought event

- Drought magnitude (M): This metric combines drought severity and duration, providing a more comprehensive picture of drought impact. It is calculated as the ratio of drought severity to drought duration, as expressed in the following Equation 7:

$$M = \frac{S}{D} \tag{7}$$

where: M represents the drought magnitude, S and D represent drought severity and duration, respectively (as defined previously).

Table 2. Drought classification according to the SDI values (Nalbantis and Tsakiris, 2009)

SDI range	Drought classification	Description
≥ 2.0	Extremely wet	Exceptionally high streamflow conditions
1.5 – 1.99	Severely wet	Streamflow conditions well above average
1.0 – 1.49	Moderately wet	Above average streamflow conditions
0.5 – 0.99	Slightly wet	Streamflow conditions near average, with a slight surplus
-0.49 – +0.49	Normal	Streamflow conditions close to the long-term average
-0.5 – -0.99	Mild drought	Below average streamflow conditions, potential for water stress
-1.0 – -1.49	Moderate drought	Significant below average streamflow conditions, water shortages likely
-1.5 – -1.99	Severe drought	Severe water deficits, agricultural impacts probable
≤ -2.0	Extremely drought	Exceptionally rare events with widespread water shortages and devastating consequences

- Relative drought frequency (*RF*): This parameter indicates the likelihood of drought occurrence within a specific timeframe. It is calculated as the ratio between the number of droughts (*n*) with negative *SDI* values within the analyzed period and the total number of drought years (*N*) considered in the analysis. The Equation 8 for relative drought frequency is:

$$RF = \frac{n}{N} \quad (8)$$

where: *RF* represents the relative drought frequency, *n* represents the number of droughts with negative *SDI* values within the analyzed period, *N* represents the total number of drought years in the analysis

By analyzing *SDI* values and their variations over time, these drought characterization metrics provide valuable insights into the frequency, intensity, and overall impact of drought events in a particular region.

Mann-Kendall trend test

The Mann-Kendall trend test is a widely used non-parametric method for detecting monotonic trends in time series data. It assesses whether a data series exhibits an increasing or decreasing monotonic trend over time. The test statistic, *S*, is calculated based on the ranks of observations in the time series. If *S* is positive, it indicates an increasing trend, while a negative *S* indicates a decreasing trend. The p-value associated with the test indicates the probability of observing such a trend if the data were random. A p-value lower than a certain threshold (generally $\alpha = 0.05$) indicates a significant trend.

Sen's slope

Sen's slope is another method used to estimate the trend in time series data. It is calculated by taking all possible pairs of data values and computing the slopes between them. The median of all these slopes is then considered as Sen's slope. Sen's slope is robust to outliers and does not require assumptions about the distribution of the data. Lower and upper bounds (generally at a 95% confidence level) are calculated to assess the significance of the slope. If the bounds do not contain zero, it indicates a significant trend.

Both these methods were employed in the study to evaluate the temporal trends of the streamflow drought index (*SDI*) in the Nekor watershed across different time scales (annual, monthly, etc.).

The Mann-Kendall trend test was used to determine if there was a significant trend towards increasing or decreasing hydrological drought over time. Sen's slope provided a quantitative estimate of the trend, along with confidence bounds to evaluate the trend's significance.

RESULTS

Annual trends in hydrological drought

An analysis of hydrological drought at the annual scale in the Nekor watershed reveals significant trends and intriguing patterns (Figure 3). The data exhibits considerable variability in the streamflow drought index (*SDI*) over 71 years, with values ranging from -1.81 to 3.016 (Table 3). This wide range reflects the diversity of hydrological conditions observed in the region over time.

Despite this variability, a marked trend emerges across the years. The Kendall's correlation coefficient (τ) calculated at -0.245 indicates a negative correlation between time and the *SDI* index, suggesting a decrease in hydrological drought over time (Table 3). This observation is corroborated by the Mann-Kendall trend test's *S* statistic, which has a value of -609, with a p-value significantly lower than $\alpha = 0.05$, thus confirming the downward trend in hydrological drought. Sen's slope, estimated at -0.018 with confidence bounds (95%) of -0.029 and -0.007, also confirms this negative trend observed in the *SDI* index (Table 3).

Hydrological trends by phase

The analysis of *SDI* values reveals distinct hydrological trends across three phases:

Phase 1: 1950–1974 (favorable streamflow conditions)

This phase was characterized by generally favorable streamflow conditions with predominantly positive *SDI* values. The minimum *SDI* of -0.81 suggests a potential dry period, but the maximum of 1.80 and a mean *SDI* of 0.5 (Slightly Wet) indicate a dominance of positive values (Table 4). The standard deviation of 0.68 reflects moderate variability in hydrological conditions during this phase (Table 4). This phase was characterized by a high frequency of wet years, with 65% (65 years) classified as surplus, indicating abundant water availability. Compared to later phases, climatic variability was relatively low during this period.

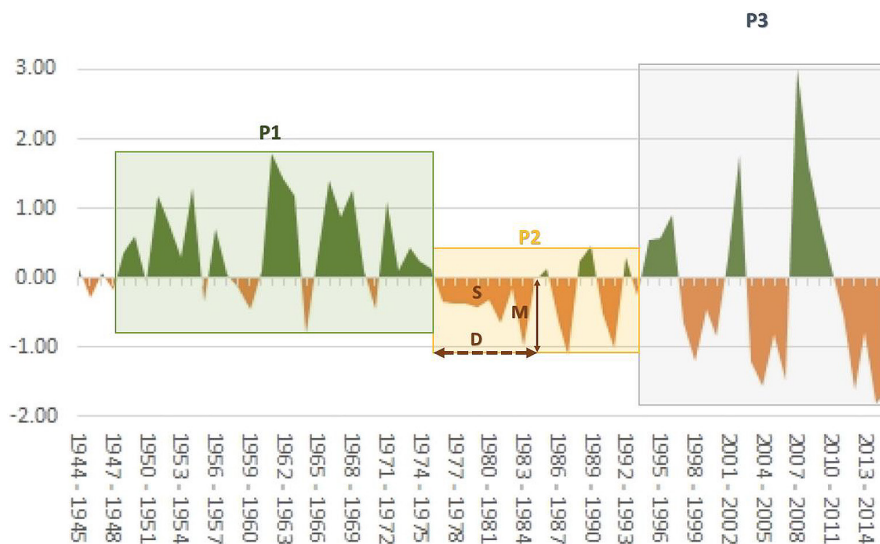


Figure 3. Annual SDI index variation at Tamellaht Station (1945–2016). P1: Phase 1: 1950–1974. P2: Phase 2: 1975–1995. P3: Phase 3: 1996–2016. D: Duration, S: Severity, M: Magnitude

Table 3. Trend analysis of standardized Runoff efficiency index values: descriptive statistics, Sen’s slope, and Mann-Kendall test results for annual values (1945–2016) at Tamellaht station

Min	Max	Average	Standard deviation	Tau de Kendall	S	Var(S)	p-value (bilatérale)	Alpha	Sen Slope
-1.815	3,016	0.032	0.920	-0.245	-609	40588	0.003	0.05	-0.018

Table 4. Drought phases: SDI (min, max, mean, and standard deviation), duration, severity, magnitude, and frequency for annual values (1945-2016) at Tamellaht station

Phase	Min	Max	Average	Standard deviation	D	S	M	RF
Phase 1	-0.81	1.80	0.5	0.68	3.00	-0.83	-0.28	0.29
Phase 2	-1.12	0.55	-0.24	0.48	11.00	-6.68	-0.61	0.70
Phase 3	-1.82	3.01	-0.26	1.30	4.00	-5.54	-1.39	0.60

The relatively low drought duration (3 years) combined with a negative but moderate severity (-0.83) and magnitude (-0.28) suggests that this phase experienced shorter and less severe drought events (Table 4). The relative drought frequency (0.29) indicates that drought occurrences were less frequent compared to wet periods (Table 4). This aligns with the characterization of this phase as years of hydrological surplus, marked by predominantly wet conditions and agricultural prosperity.

The favorable hydrological conditions supported increased agricultural productivity. Crop yields in quintals per hectare for the Temsamane and Bni Touzine tribes, particularly during the 1960s (e.g., 1963/64, 1967/68, 1968/69), highlight this positive trend (Figure 4). This period of agricultural prosperity and stability likely contributed to the socio-economic development of

the region. The low climatic variability provided a predictable environment for agricultural activities, promoting the well-being of communities dependent on agriculture.

Phase 2: 1975–1995 (increased hydrological stress)

This phase witnessed a shift towards hydrological deficits, with predominantly negative SDI values indicative of drought conditions. The minimum SDI of -1.12 is less negative than Phase 1, but the maximum SDI of 0.56 is less significant, suggesting a decline in high flow events (Table 4). The mean SDI of -0.24 (close to zero but slightly negative) reflects the prevalence of negative values (Table 4). The standard deviation of 0.48 is lower compared to Phase 1, suggesting lower

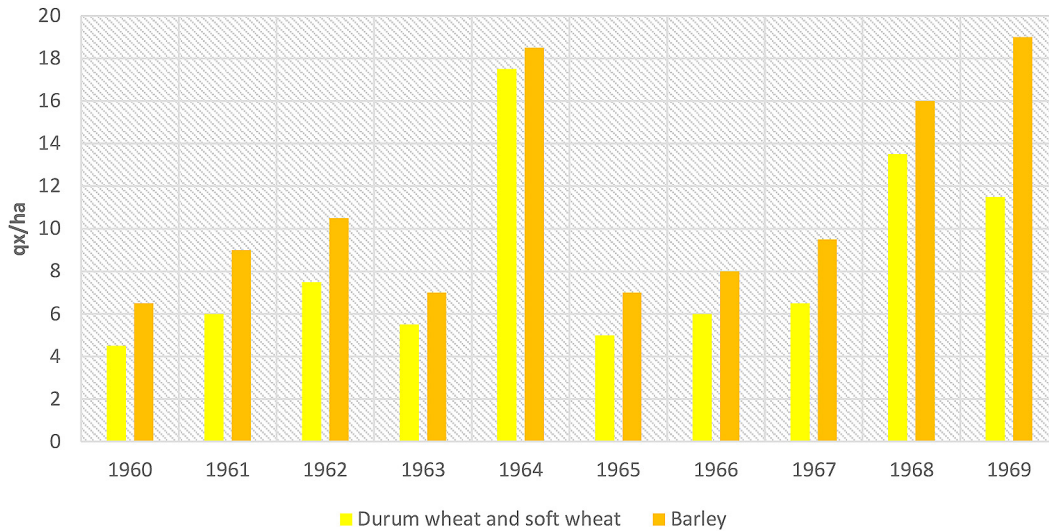


Figure 4. Evolution of crop yields in quintals per hectare in the Tamsamane and Bni Touzine tribes between 1960 and 1969 (Northeast of the Nekor watershed), Bossard [1978]

variability in hydrological conditions, potentially with more frequent or severe drought events.

This phase is characterized by a significantly longer drought duration (11 years) compared to Phase 1, indicating prolonged and recurrent drought events (Table 4). The high drought severity (-6.68) and magnitude (-0.61) suggest severe and impactful drought conditions during this period (Table 4). The high relative drought frequency (0.7, accounting for 80%) indicates that drought occurrences were frequent and dominant, reflecting the recurrence of drought years and their profound effects on water resources, agriculture, and socio-economic activities. This phase witnessed a significant shift towards hydrological deficits, characterized by an extended period of reduced

precipitation. While the analysis of hydrological drought indices reveals alternating deficit and surplus years, the 1980s were particularly severe. This decade saw a high frequency of dry years. The peak intensity occurred during the 1983/1984 agricultural year, with a recorded value of -0.79 on a SDI. Conversely, surplus years were scarce, constituting only 20% of this phase (3 years).

The increased frequency and intensity of droughts significantly impacted the agricultural sector in the study area. This challenging period resulted in a dramatic decline in crop production, yields, and livestock numbers. For instance, goat populations decreased by 56.56% between 1978 and 1983 (Figure 5), highlighting the severity of the impact.

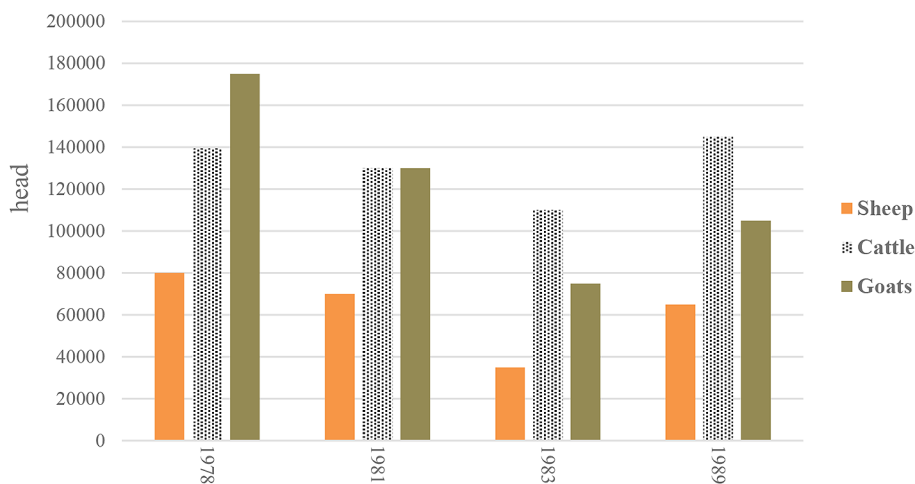


Figure 5. Evolution of livestock population in the province of Al Hoceima (1978–1989), El Sabri [1995]

The Eastern Rif Folded Mountains, a region steeped in history and once characterized by high population densities, witnessed a significant demographic shift during the 1980s. This transformation was inextricably linked to a series of severe drought years that gripped the region.

The succession of drought years in the 1980s proved to be a formidable challenge for the inhabitants of the Eastern Rif Folded Mountains. The scarcity of water and the resulting decline in agricultural productivity had a profound impact on livelihoods and living conditions. Faced with these hardships, many families were compelled to seek alternative means of sustenance and opportunities beyond their traditional mountain homes.

Rural exodus, fueled by the persistent drought conditions, became a defining feature of the region during the 1980s. As individuals and families sought better prospects in neighboring towns and cities, the once-bustling mountain communes experienced a steady decline in population. This depopulation was particularly pronounced in areas with limited natural resource potential, such as the commune of Arbaa Taourirt, which witnessed a staggering 32% population decrease between 1982 and 2014 (Table 5).

The impact of the 1980s drought and the subsequent rural exodus continues to resonate in the Eastern Rif Folded Mountains today. The region’s once-high population densities have given way to lower numbers, particularly in mountainous areas. This demographic shift has had far-reaching consequences for the social, economic, and cultural fabric of the region.

The intensified hydrological drought during Phase 2 had substantial negative consequences

for agriculture and potentially contributed to other socio-economic challenges in the region. Future water resource management strategies need to consider the possibility of recurring droughts to ensure the resilience of the agricultural sector and the livelihoods of local communities.

Phase 3: 1996–2016 (high hydrological variability)

This phase exhibits significant fluctuations in SDI values, reflecting a period of changing hydrological conditions. The minimum SDI of -1.81 (Extremely drought) and maximum SDI of 3.01 (Extremely wet) represent a wider range compared to previous phases (Table 4). The mean SDI of -0.26 remains close to zero. However, the high standard deviation of 1.30 suggests a considerable level of hydrological variability during this phase, with both wet and dry periods likely occurring (Table 4). This variability highlights the dynamic nature of hydrological processes within the Nekor watershed.

In this phase, the drought duration (4 years) is shorter compared to Phase 2 but longer than Phase 1, indicating a moderate duration of drought events. The drought severity (-5.54) and magnitude (-1.39) are both high, signifying severe and impactful drought conditions similar to Phase 2 (Table 4). The relative drought frequency (0.60) suggests frequent drought occurrences, although slightly lower compared to Phase 2 (Table 4). The high variability in drought characteristics reflects the dynamic and fluctuating nature of hydrological conditions during this period.

This phase is characterized by significant fluctuations in hydrological conditions, as evidenced by the analysis of drought indices. The intensity

Table 5. Population and household evolution in Arbaa Taourirt commune, 1960–2014, including annual growth rate

Description		Headcount	Annual growth rate in %
1960	Population	10445	***
1971	Population	13146	2.1
	Households	2455	***
1982	Population	16191	1.9
	Households	2565	***
1994	Population	8110	-5.5
	Households	1279	***
2004	Population	7272	-1.1
	Households	1156	***
2014	Population	5187	-3.3
	Households	985	***

Note: *** Data not available. Based on the results of the General Population and Housing Census.

of dry and wet years varied considerably, with the driest year (-1.17 in 2013–2014, categorized as moderately dry) and the wettest year (+4.75 in 2008, categorized as extremely wet) showcasing this extreme variability (Table 4). This variability resulted in contrasting extreme events, such as the devastating October 2008 floods and the agricultural drought of 2013–2014.

The 2013–14 drought caused significant agricultural losses, with a 65.7% decrease in barley yield (from 17.2 quintals/hectare to 5.9 quintals/hectare) (Figure 6). Losses in durum wheat and soft wheat were also observed, although less severe.

The high hydrological variability of Phase 3 had a notable impact on the region’s demographics. The Eastern Rif’s mountainous areas experienced a decline in population density due to rural exodus, likely triggered by the adverse effects of droughts. Population density decreased from 57 inhabitants/km² in 1994 to 34 inhabitants/km² in 2014 (Table 6). Conversely, urban centers, particularly Bni Bouayach, witnessed rapid population growth (11.9% from

1982 to 1994), likely due to migration from rural areas seeking better opportunities. The population of Bni Bouayach Agglomeration, the largest locality in the watershed, nearly quadrupled during this period (from 4,253 in 1982 to 18,271 in 2014) (Table 6). This rapid urbanization placed pressure on basic services and infrastructure.

Monthly trends in hydrological drought

The analysis of the Sen’s Slope and Kendall’s tau values for each month reveals varying trends in hydrological drought across the year in the Nekor watershed. Here’s a breakdown of the results:

- Months with increasing trends: August ($\tau = 0.356$, p-value < 0.0001, Sen’s slope = 0.010) and September ($\tau = 0.310$, p-value < 0.0001) exhibit a statistically significant increasing trend in hydrological drought according to both Kendall’s tau and Sen’s slope. This indicates a tendency for droughts to become more severe over time during these months (Table 7).

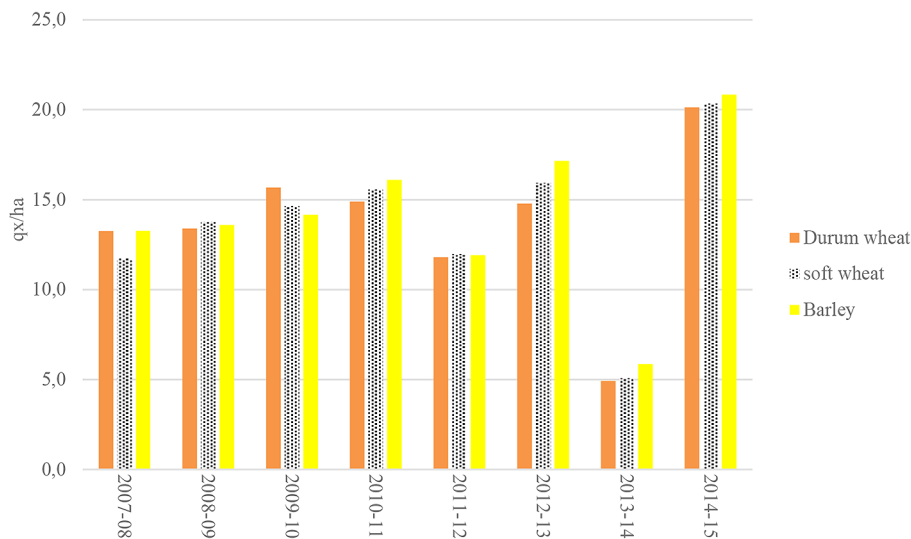


Figure 6. Evolution of crop yields in quintals per hectare in the province of Al Hoceima between 2007 and 2014 (Regional Directorate of Tanger-Tétouan-Al Hoceima)

Table 6. Evolution of population, households, and population densities (inhabitants/km²) in the topographic units of the Nekor watershed, 1994–2014.

Description	1994			2004			2014		
	Population	Households	Density	Population	Households	Density	Population	Households	Density
Hills, and low mountains	40237	6411	120	40451	6914	121	41784	8450	125
High folded mountains	32997	5260	57	24814	4196	43	19759	3390	34
Nekor watershed total	73234	11671	80	65265	11110	71	61543	11840	67
Bni Bouayach commune	13128	2255	577	15497	2956	681	18271	4062	803

Note: Based on the results of the General Population and Housing Census (RGPH) 1994–2014.

- Months with no clear trend (Table 7): July ($\tau = 0.067$, $p\text{-value} = 0.427$) and October ($\tau = 0.072$, $p\text{-value} = 0.384$) have tau values close to zero, along with non-significant p-values, suggesting no statistically significant trend.
- Months with decreasing trends (Table 7): The remaining months (December to July, and May) display negative tau values. Among these:
 - April ($\tau = -0.309$, $p\text{-value} = 0.0001$) and May ($\tau = -0.321$, $p\text{-value} < 0.0001$) have statistically significant negative tau values and p-values much lower than 0.05, indicating a strong decreasing trend in hydrological drought according to Kendall's tau. Sen's slope values are also negative for these months, further supporting this observation.
 - January ($\tau = -0.194$, $p\text{-value} = 0.017$), March ($\tau = -0.174$, $p\text{-value} = 0.033$), December ($\tau = -0.081$, $p\text{-value} = 0.323$), February ($\tau = -0.114$, $p\text{-value} = 0.160$), and Jun ($\tau = -0.163$, $p\text{-value} = 0.045$) show weaker evidence for decreasing trends. While the tau values are negative, some p-values are not significant at the 0.05 level.

In short, the analysis reveals a pattern of decreasing hydrological drought trends throughout the spring months (February to May). Conversely, September shows an increasing trend, indicating a potential rise in drought severity during that month. September and the remaining winter months (November to January) require further investigation to solidify the trends. Kendall's Tau

values indicate significant climatic variations within the models. For September, a value of 0.31 is observed (Table 7), This indicates the late arrival of autumn rains. Conversely, the May equivalent exhibits a value of -0.32 (Table 7), suggesting rainfall patterns less conducive to agriculture as they occur after the harvest season. These findings underscore the dynamic nature of climatic conditions within the studied models.

Seasonal trends in hydrological drought

The analysis of Kendall's tau, p-value, and Sen's slope values reveals varying trends in hydrological drought across the seasons defined by the hydrological year in Morocco (September to August).

- Season 1 (September to November) (Table 8): This season exhibits a weak positive trend in hydrological drought ($\tau = 0.106$, $p\text{-value} = 0.193$). The Kendall's tau value suggests a weak positive correlation between time and the SDI, indicating a slight increase in drought severity over the years. However, the high p-value (0.193) indicates that this trend is not statistically significant. The Sen's slope of 0.008 further supports this by showing a minimal positive trend.
- Season 2 (December to February) (Table 8): There is a statistically significant negative trend in hydrological drought for Season 2 ($\tau = -0.172$, $p\text{-value} = 0.034$). The Kendall's tau value indicates a weak negative correlation between time and the SDI, suggesting a decrease in drought severity over the years.

Table 7. Trend analysis of standardized runoff efficiency index (SDI) values: descriptive statistics, Sen's slope, and Mann-Kendall test results for each month (1945–2016) at Tamellaht station

Month	Min	Max	Average	Standard deviation	Tau de Kendall	S	Var(S)	p-value (bilatérale)	alpha	Sen Slope
Sep	-0,579	2,619	0,174	0,776	0,31	712	38281	<0.0001	0,05	0,006
Oct	-0,144	2,850	0,534	0,520	0,072	176	40455	0,384	0,05	0,003
Nov	-0,688	2,961	0,379	0,599	0,034	85	40568	0,677	0,05	0,002
Dec	-2,287	2,181	-0,002	0,996	-0,081	-200	40585	0,323	0,05	-0,006
Jan	-2,282	2,298	-0,010	1,014	-0,194	-482	40581	0,017	0,05	-0,015
Feb	-2,406	2,538	0,036	0,939	-0,114	-284	40585	0,16	0,05	-0,009
Mar	-1,539	2,527	0,070	0,878	-0,174	-431	40582	0,033	0,05	-0,012
Apr	-2,765	2,164	-0,099	1,172	-0,309	-767	40582	0,0001	0,05	-0,023
May	-2,303	2,805	0,071	0,897	-0,321	-796	40583	<0.0001	0,05	-0,021
Jun	-1,703	2,360	-0,002	0,991	-0,163	-404	40560	0,045	0,05	-0,013
Jul	-0,756	2,922	0,140	0,813	0,067	159	39602	0,427	0,05	0,001
Aug	-0,518	2,584	0,185	0,749	0,356	816	38261	<0.0001	0,05	0,01

This is confirmed by the low p-value (0.034), which signifies a statistically significant trend. The Sen’s slope of -0.013 further confirms this downward trend in drought severity.

- Season 3 (March to May) (Table 8): Season 3 displays a highly significant negative trend in hydrological drought ($\tau = -0.337$, p-value < 0.0001). The strong negative correlation indicated by the Kendall’s tau value suggests a substantial decrease in drought severity over the years. The very low p-value (< 0.0001) confirms the statistical significance of this trend. The Sen’s slope of -0.025 further underscores this considerable downward trend.
- Season 4 (June to August) (Table 8): No statistically significant trend in hydrological drought is observed for Season 4 ($\tau = -0.059$, p-value = 0.472). The Kendall’s tau value suggests a slight negative correlation between time and the SDI, indicating a minor decrease in drought severity over the years. However, the high p-value (0.472) indicates that this trend is not statistically significant. The Sen’s slope of -0.005 further confirms the absence of a significant trend in drought severity for this season.

In summary, Season 3 (March to May) exhibits the strongest statistically significant negative trend in hydrological drought, indicating a substantial decrease in drought severity over time. Season 2 (December to February) also shows a statistically significant negative trend, although weaker than Season 3. Season 4 (June to August) does not exhibit a statistically significant trend, and Season 1 (September to November) shows a weak, non-significant tendency towards increasing drought severity.

DISCUSSION

The current study employed the SDI index to investigate drought trends and patterns over an extended period (1945–2016) and across different time scales (monthly, seasonal, annual). Unlike

previous studies that often focused solely on annual trends, this study examined drought patterns in terms of duration, severity, magnitude, and frequency for each phase.

For example, a study by Benyoussef et al. [2024] based on SPI, RDI, and DI indices identified a relatively long period of 38 years (1978–2016) with a general increase in annual rainfall during that period. However, this increase might be explained by the studied period coinciding with the beginning of a dry spell followed by years of climatic variability.

Another study conducted in the Ghis-Nekor plain by Larabi et al. [2020] identified an annual drought trend and period using the SPI index for the years 1964 to 2014. This study found a seven-year dry period from 1980 to 1987. In contrast, the current study identified a slightly longer drought period of 11 years from 1977 to 1988 in the Nekor watershed. This difference is likely attributed to the fact that hydrological droughts typically last longer than meteorological droughts, primarily due to the basin’s physical characteristics. This finding aligns with Van Loon et al. [2016], who noted that factors such as soil type, lithology, and land use can influence a basin’s hydrological response to climate variability.

In their study of the Upper Indus Basin in Pakistan, Saifullah et al. [2021] employed a threshold approach to analyze drought events, scarcity, and duration. They aimed to determine spatio-temporal patterns of hydrological droughts from 1961 to 2010. The study observed a significant increase in the maximum duration of drought events at Naran, with a slight increase in the extreme pattern of the maximum drought duration. However, the same study identified decreasing trends in the maximum duration of hydrological droughts at Garhi Habibullah.

As previously mentioned, ecosystems respond differently to meteorological and hydrological droughts. This variation depends on several factors, including vegetation type [Flach et al., 2018;

Table 8. Trend analysis of standardized runoff efficiency index values: descriptive statistics, Sen’s slope, and Mann-Kendall test results for each season (1945–2016) at Tamellaht Station

Season	Min	Max	Average	Standard deviation	Tau de Kendall	S	Var(S)	p-value (bilatérale)	alpha	Sen Slope
Season 1	-0.83	2.860	0.302	0.610	0,106	263	40584	0,193	0,05	0,008
Season 2	-1,60	2,680	0,027	0,939	-0,172	-428	40587	0,034	0,05	-0,013
Season 3	-1,968	2,081	-0,004	1,007	-0,337	-837	40588	<0.0001	0,05	-0,025
Season 4	-2,015	2,882	0,027	0,964	-0,059	-146	40568	0,472	0,05	-0,005

Lian et al., 2020], soil properties [Bastos et al., 2020; Pittelkow et al., 2015], and microclimate conditions [Suarez and Kitzberger, 2008]. Management practices [Acevedo et al., 2020], pre-drought conditions [Laaha et al., 2017; Van Loon et al., 2015], and the timing of drought within the growing season [Van Lanen et al., 2016] also significantly influence these responses.

The current study demonstrates a negative trend in hydrological drought over time, as indicated by Kendall's τ (-0.245), the Mann-Kendall test, and Sen's slope (-0.018). This decline in hydrological drought can be linked to an increase in severe weather patterns, which is further confirmed by the standard deviation values of each phase (phase 1: SD = 0.68, phase 2: SD = 0.48, and phase 3: SD = 1.30). With rainfall becoming more concentrated over shorter durations, this phenomenon leads to floods and elevated daily and monthly flow rates in specific years. However, despite this intensified precipitation pattern, drought persists, as indicated by the findings of the Kendall's correlation coefficient and Sen's slope correlation results. Similar patterns were observed by Rahmani and Fattahi [2024] in a study conducted in central England, United Kingdom, investigating alterations in drought and flood occurrences due to climate change. The findings suggest that climate change has amplified the likelihood of river flooding in recent years, while the occurrences of annual droughts and wet conditions remain unaffected by climate change. Another study conducted by Kazemzadeh and Malekian [2016] observed a decreasing trend in the spatial and temporal characteristics of hydrological drought, particularly over the last three decades in Iran. Similarly, Yilmaz [2019] found a decreasing trend in hydrological drought in southeastern Turkey, predicting a severe drought will hit this region in the near future. Our findings and those of other studies diverged slightly from those reported for Cyprus [Myronidis et al., 2018, where hydrological drought trends appeared to intensify over time.

Studies by Bouras et al. [2019] in Morocco highlight the significant impacts of climate change on the Tensift region. Their findings suggest a decrease in autumn rainfall, potentially making later sowing dates preferable under a changing climate. Similarly, regional studies by Trigo and Palutikof [2001] analyzing precipitation scenarios over the Iberian Peninsula revealed an increase in winter precipitation and a decrease

in autumn precipitation using various downscaling techniques. The current study on the Nekor basin further strengthens the evidence for a decrease in autumn rainfall (September-October-November) and the recurrence of droughts with increasing climate variability.

Since 2005, many residents of the Nekor plain have reported a significant reduction in water resources allocated to agriculture due to declining water availability, which is partially attributed to the effects of hydrological drought. Decreased water pump capacity and increased sedimentation in water reservoirs have directly impacted the agricultural water supply, leading to reduced irrigation opportunities and agricultural output, characteristic of hydrological drought impacts [Okacha et al., 2023].

This reduction in water resources has profoundly affected agricultural activities, with farmers reporting decreases in crop yields and income. Multiple factors, including successive years of drought, reduced water availability, and soil salinity, have led to significant changes in agricultural practices [Okacha, 2020]. These changes are directly related to the impact of hydrological drought, which manifests as decreased water availability for irrigation and increased soil aridity, thus affecting agricultural productivity. Recurring drought and excessive heat exacerbate hydrological drought conditions by increasing evaporation rates and decreasing precipitation [Machrafi et al., 2022]. These climatic factors further reduce water availability for agriculture, worsening the impacts of hydrological drought on agricultural productivity and rural livelihoods.

Consequently, the population has increasingly shifted to non-agricultural activities, such as construction and trade, as reported by many local residents. This shift can be attributed to the economic impacts of hydrological drought on agriculture. Decreased agricultural productivity and livelihood insecurity due to water scarcity have likely prompted individuals to seek alternative sources of income, indirectly influenced by the hydrological drought's effects on agricultural water resources.

CONCLUSIONS

The Nekor Watershed in northeastern Morocco faces significant challenges due to pronounced climatic variability and increasing hydrological droughts. This study investigated

long-term (1945–2016) drought patterns and trends, focusing on their impacts on agriculture and population distribution.

The analysis revealed substantial climate fluctuations, with distinct dry and wet periods. Season 1 (September–November) showed a weak, non-significant trend towards increasing drought severity. Conversely, Season 3 (March–May) displayed a statistically significant trend towards less severe droughts, suggesting a shift in rainfall patterns. This trend aligns with the broader context of climate change, where alterations in precipitation patterns are becoming increasingly evident.

While summer months might experience increased streamflow due to thunderstorms or flooding, as indicated by the positive association with August, this doesn't necessarily alleviate drought concerns. These events are often short-lived and have minimal impact on long-term water storage. Conversely, the negative association with May highlights a concerning trend towards drier conditions during the crucial agricultural production period. Rainfall occurring after harvest offers minimal benefit and can exacerbate drought concerns.

The most concerning finding is the observed trend towards increasing hydrological droughts, particularly in recent decades. This finding aligns with historical data documenting rural exodus from the surrounding mountains during this period. Water scarcity and declining agricultural productivity likely pushed families to seek alternative opportunities. The case of Arbaa Taourirt, with a dramatic population decline, exemplifies the impact of drought on population distribution.

The urgency of implementing proactive water management strategies in the Nekor Watershed is paramount. Embracing adaptive measures and promoting sustainable practices are crucial for enhancing regional resilience and safeguarding livelihoods in the face of a changing climate.

Acknowledgments

The authors are grateful for the data support provided by the Hydraulic Basin Agencies and the National Meteorological Directorate. Deep thanks and gratitude to the Researchers Supporting Project Number (RSP2024R351), King Saud University, Riyadh, Saudi Arabia, for funding this research article.

REFERENCES

1. Abdelmajid, S., Mukhtar, A., Baig, M.B., Reed, M.R. 2021. Climate change, agricultural policy and food security in Morocco. *Emerging Challenges to Food Production and Security in Asia, Middle East, and Africa: Climate Risks and Resource Scarcity*, 171–196. https://doi.org/10.1007/978-3-030-72987-5_7
2. Acevedo, M., Pixley, K., Zinyengere, N., Meng, S., Tufan, H., Cichy, K., Bizikova, L., Isaacs, K., Ghezzi-Kopel, K., Porciello, J. 2020. A scoping review of adoption of climate-resilient crops by small-scale producers in low-and middle-income countries. *Nature plants* 6, 1231–1241. <https://doi.org/10.1038/s41477-020-00783-z>
3. Amouch, S., and Akhssas, A. 2023. Drought variability in Agadir's Region (Southern Morocco) – Recent and future trends. *Ecological Engineering & Environmental Technology* 24, 241–250. <https://doi.org/10.12912/27197050/157169>
4. Bastos, A., Ciais, P., Friedlingstein, P., Sitch, S., Pongratz, J., Fan, L., Wigneron, J.-P., Weber, U., Reichstein, M., Fu, Z. 2020. Direct and seasonal legacy effects of the 2018 heat wave and drought on European ecosystem productivity. *Science advances* 6, eaba2724. <https://doi.org/10.1126/sciadv.aba2724>
5. Ben-Zvi, A. 1987. Indices of hydrological drought in Israel. *Journal of hydrology* 92, 179–191
6. Benyoussef, S., Arabi, M., El Yousfi, Y., Cheikh, B.B., Abdaoui, A., Azirar, M., Mechkirrou, L., El Ouarghi, H., Zegzouti, Y.F., Boughrous, A.A. 2024. Climate change and water resources management in the Ghis-Nekor watershed (North of Morocco)—A comprehensive analysis using SPI, RDI and DI Indices. *Ecological Engineering & Environmental Technology* 25. <https://doi.org/10.12912/27197050/176275>
7. Bossard, R. 1978. Mouvements migratoires dans le Rif oriental: le travail en Europe. Aspect contemporain majeur des migrations dans la province de Nador, Université Paul Valéry-Montpellier III
8. Bouras, E., Jarlan, L., Khabba, S., Er-Raki, S., Dezetter, A., Sghir, F., Trambly, Y. 2019. Assessing the impact of global climate changes on irrigated wheat yields and water requirements in a semi-arid environment of Morocco. *Scientific reports* 9, 19142. <https://doi.org/10.1038/s41598-019-55251-2>
9. De Martonne, E. 1923. Aridité et indices d'aridité. *Académie des Sciences. Comptes Rendus* 182, 1935-1938
10. Değerli Şimşek, S., Çapar, Ö. F., Turhan, E. 2023. Investigation of transition possibilities between drought classifications using standardized precipitation index for wet and dry periods – Lower Seyhan Plain, Türkiye case. *Journal of Ecological Engineering* 24, 201-209. <https://doi.org/10.12912/27197050/157169>

- org/10.12911/22998993/161655
11. El Sabri, S. 1995. Approche du phenomene de la croissance urbaine dans le Rif Central (Province d'Al Hoceima, Nord du Maroc): cas du doublet Imzouren-Bni Bouayach. Thèse Doct, van Amsterdam, Faculty of Social and Behavioural Sciences (FMG), Amsterdam, Pays-Bas
 12. Elair, C., Rkha Chaham, K., Hadri, A. 2023. Assessment of drought variability in the Marrakech-Safi region (Morocco) at different time scales using GIS and remote sensing. *Water Supply* 23, 4592–4624. <https://doi.org/10.2166/ws.2023.283>
 13. Fan, G., Zhang, Y., He, Y., Wang, K. 2017. Risk assessment of drought in the Yangtze River Delta based on natural disaster risk theory. *Discrete Dynamics in Nature and Society* 2017. <https://doi.org/10.1155/2017/5682180>
 14. Flach, M., Sippel, S., Gans, F., Bastos, A., Brenning, A., Reichstein, M., Mahecha, M.D. 2018. Contrasting biosphere responses to hydrometeorological extremes: revisiting the 2010 western Russian heatwave. *Biogeosciences* 15, 6067–6085
 15. Gaaloul, N., Eslamian, S., Katlance, R. 2021. Impacts of climate change and water resources management in the southern mediterranean countries. *Water Productivity Journal* 1, 51–72. <https://doi.org/10.22034/wpj.2020.119476>
 16. Kazemzadeh, M., Malekian, A. 2016. Spatial characteristics and temporal trends of meteorological and hydrological droughts in northwestern Iran. *Natural Hazards* 80, 191–210
 17. Laaha, G., Gauster, T., Tallaksen, L.M., Vidal, J.-P., Stahl, K., Prudhomme, C., Heudorfer, B., Vlnas, R., Ionita, M., Van Lanen, H.A. 2017. The European 2015 drought from a hydrological perspective. *Hydrology and Earth System Sciences* 21, 3001–3024
 18. Larabi, A., El Asri, H., El Hamidi, M., Zhim, S., Faouzi, M. 2020. Climate change trends in Morocco's Mediterranean & Atlantic Hydraulic Basins: Impacts on water resources. *Int J Water Resour Arid Environ* 9, 01–20
 19. Li, Y., Johnson, E. J., and Zaval, L. 2011. Local warming: Daily temperature change influences belief in global warming. *Psychological science* 22, 454–459
 20. Lian, X., Piao, S., Li, L. Z., Li, Y., Huntingford, C., Ciais, P., Cescatti, A., Janssens, I.A., Peñuelas, J., Buermann, W. 2020. Summer soil drying exacerbated by earlier spring greening of northern vegetation. *Science advances* 6, eaax0255
 21. Machrafi, O., Sguigaa, A., Attou, A., Sabir, M., Naimi, M., Chikhaoui, M. 2022. Analysis of the water management system in a mountain territory, the case of the Nekor Watershed, Rif, Morocco. *Open Journal of Modern Hydrology* 12, 125–154. <https://doi.org/10.4236/ojmh.2022.124008>
 22. Maybank, J., Bonsai, B., Jones, K., Lawford, R., O'Brien, E., Ripley, E., Wheaton, E. 1995. Drought as a natural disaster. *Atmosphere-Ocean* 33, 195–222. <https://doi.org/10.1080/07055900.1995.9649532>
 23. McKee, T.B., Doesken, N.J., Kleist, J. 1993. The relationship of drought frequency and duration to time scales. In "Proceedings of the 8th Conference on Applied Climatology", 17, 179–183. California.
 24. Meliho, M., Khattabi, A., Jobbins, G., Sghir, F. 2020. Impact of meteorological drought on agriculture in the Tensift watershed of Morocco. *Journal of Water and Climate Change* 11, 1323–1338. <https://doi.org/10.2166/WCC.2019.279>
 25. Modarres, R. 2007. Streamflow drought time series forecasting. *Stochastic Environmental Research and Risk Assessment* 21, 223–233
 26. Myronidis, D., Ioannou, K., Fotakis, D., Dörflinger, G. 2018. Streamflow and hydrological drought trend analysis and forecasting in Cyprus. *Water resources management* 32, 1759–1776. DOI: 10.1007/s11269-018-1902-z
 27. Nalbantis, I., Tsakiris, G. 2009. Assessment of hydrological drought revisited. *Water resources management* 23, 881–897. <https://doi.org/10.1007/s11269-008-9305-1>
 28. Okacha, A. 2020. Effet des transformations territoriales et des contraintes climatiques sur les modalites de gestion du risque d'inondation dans le bassin versant de nekkor. Thèse Doct, Abdelmalek Essaadi, Faculté des lettres et sciences humaines de Tétouan, Maroc
 29. Okacha, A., Salhi, A., Arari, K., El Badaoui, K., Lahrichi, K. 2023. Soil erosion assessment using the RUSLE model for better planning: a case study from Morocco. *Modeling Earth Systems and Environment*, 1–9. <https://doi.org/10.1007/s40808-023-01731-4>
 30. Okacha, A., Salhi, A., Arari, K., El Badaoui, K., Lahrichi, K. 2023. Soil erosion assessment using the RUSLE model for better planning: A case study from Morocco. *Modeling Earth Systems and Environment* 9, 3721–3729
 31. Pittelkow, C.M., Linquist, B.A., Lundy, M.E., Liang, X., Van Groenigen, K.J., Lee, J., Van Gestel, N., Six, J., Venterea, R.T., Van Kessel, C. 2015. When does no-till yield more? A global meta-analysis. *Field crops research* 183, 156–168. <https://doi.org/10.1016/j.fcr.2015.07.020>
 32. Polevoy, A., Barsukova, O., Husieva, K., Zhygai-lo, O., Volvach, O., Kyrnasivska, N., Tolmachova, A., Zhygai-lo, T., Danilova, N., Kostyukievych, T. 2024. The climate change impact on the development of droughts in Ukraine. *Journal of Ecological Engineering* 25, 194–205. <https://doi.org/10.12911/22998993/187276>
 33. Qaisrani, A., Umar, M.A., Siyal, G.E.A., Salik, K.M. 2018. What defines livelihood vulnerability in rural semi-arid areas? Evidence from Pakistan.

- Earth Systems and Environment 2, 455–475
34. Rahmani, F., Fattahi, M.H. 2024. Investigation of alterations in droughts and floods patterns induced by climate change. *Acta Geophysica* 72, 405–418. <https://doi.org/10.1007/s11600-023-01043-2>
 35. Redner, S., and Petersen, M.R. 2006. Role of global warming on the statistics of record-breaking temperatures. *Physical Review E* 74, 061114
 36. Saifullah, M., Liu, S., Adnan, M., Zaman, M., Muhammad, S., Babur, M., Zhu, Y., Wu, K. 2021. Assessment of spatial and temporal pattern of hydrological droughts in the upper indus basin, Pakistan. *Polish Journal of Environmental Studies* 30, 4633–4645
 37. Salhi, A., Martin-Vide, J., Benhamrouche, A., Benabdelouahab, S., Himi, M., Benabdelouahab, T., Casas Ponsati, A. 2019. Rainfall distribution and trends of the daily precipitation concentration index in northern Morocco: A need for an adaptive environmental policy. *SN Applied Sciences* 1, 1–15. <https://doi.org/10.1007/s42452-019-0290-1>
 38. Serrano, S.V., Begueria, S., Moreno, J.L. 2010. A multiscalar drought index sensitive to global warming: The standardized precipitation evapotranspiration index. *Journal of Climate* 23, 1696–1718
 39. Snaibi, W., Mezrhab, A., Sy, O., Morton, J.F. 2021. Perception and adaptation of pastoralists to climate variability and change in Morocco's arid rangelands. *Heliyon* 7. <https://doi.org/10.1016/j.heliyon.2021.e08434>
 40. Sridhar, V., Hubbard, K.G., You, J., Hunt, E.D. 2008. Development of the soil moisture index to quantify agricultural drought and its "user friendliness" in severity-area-duration assessment. *Journal of Hydrometeorology* 9, 660–676
 41. Staudinger, M., Stahl, K., Seibert, J. 2014. A drought index accounting for snow. *Water Resources Research* 50, 7861–7872. <https://doi.org/10.1002/2013WR015143>
 42. Suarez, M.L., Kitzberger, T. 2008. Recruitment patterns following a severe drought: Long-term compositional shifts in Patagonian forests. *Canadian Journal of Forest Research* 38, 3002–3010
 43. Thornthwaite, C.W. 1948. An approach toward a rational classification of climate. *Geographical review* 38, 55–94
 44. Trigo, R.M., Palutikof, J.P. 2001. Precipitation scenarios over Iberia: A comparison between direct GCM output and different downscaling techniques. *Journal of Climate* 14, 4422–4446
 45. Van Lanen, H.A., Laaha, G., Kingston, D.G., Gauster, T., Ionita, M., Vidal, J.-P., Vlnas, R., Tallaksen, L.M., Stahl, K., Hannaford, J. 2016. Hydrology needed to manage droughts: the 2015 European case. *Hydrological Processes* 30, 3097–3104. <https://dx.doi.org/10.1002/hyp.10838>
 46. Van Loon, A.F., Ploum, S., Parajka, J., Fleig, A., Garnier, E., Laaha, G., Van Lanen, H. 2015. Hydrological drought types in cold climates: quantitative analysis of causing factors and qualitative survey of impacts. *Hydrology and Earth System Sciences* 19, 1993–2016. <https://doi.org/10.5194/hess-19-1993-2015>
 47. Van Loon, A.F., Stahl, K., Di Baldassarre, G., Clark, J., Rangelcroft, S., Wanders, N., Gleeson, T., Van Dijk, A.I., Tallaksen, L.M., Hannaford, J. 2016. Drought in a human-modified world: Reframing drought definitions, understanding, and analysis approaches. *Hydrology and Earth System Sciences* 20, 3631–3650. <https://doi.org/10.5194/hess-20-3631-2016>
 48. Yilmaz, B. 2019. Analysis of hydrological drought trends in the gap region (Southeastern Turkey) by Mann-Kendall test and innovative Şen method. *Applied Ecology & Environmental Research* 17. http://dx.doi.org/10.15666/aeer/1702_33253342
 49. Zahour, M. 2021. Food security in Morocco: Risk factors and governance. *Emerging Challenges to Food Production and Security in Asia, Middle East, and Africa: Climate risks and resource scarcity*, 149–170. https://doi.org/10.1007/978-3-030-72987-5_6
 50. Zaidman, M., Rees, H., Young, A. 2002. Spatio-temporal development of streamflow droughts in north-west Europe. *Hydrology and Earth System Sciences* 6, 733–751
 51. Zhou, S., Wang, Y., Chang, J., Su, H., Huang, Q., Li, Z. 2024. Quantifying the effects of future environmental changes on water supply and hydropower generation benefits of cascade reservoirs in the Yellow River Basin within the framework of reservoir water supply and demand uncertainty. *Journal of Hydrology: Regional Studies* 52, 101729. <https://doi.org/10.1016/j.ejrh.2024.101729>